Published in final edited form as:
ASAIO J. 2008 ; 54(1): 64–72. doi:10.1097/MAT.0b013e31815d6898.

Platelet Activation Due to Hemodynamic Shear Stresses: Damage Accumulation Model and Comparison to *In Vitro* Measurements

Matteo Nobili[*], **Jawaad Sheriff**[†], **Umberto Morbiducci**[‡], **Alberto Redaelli**[*], and **Danny Bluestein**[†]

[*] Department of Bioengineering, Politecnico di Milano, Milan, Italy

[†] Department of Biomedical Engineering, Stony Brook University, Stony Brook, New York

[‡] Department of Mechanics, Polytechnic University of Turin, Turin, Italy

Abstract

The need to optimize the thrombogenic performance of blood recirculating cardiovascular devices, *e.g.*, prosthetic heart valves (PHV) and ventricular assist devices (VAD), is accentuated by the fact that most of them require lifelong anticoagulation therapy that does not eliminate the risk of thromboembolic complications. The formation of thromboemboli in the flow field of these devices is potentiated by contact with foreign surfaces and regional flow phenomena that stimulate blood clotting, especially platelets. With the lack of appropriate methodology, device manufacturers do not specifically optimize for thrombogenic performance. Such optimization can be facilitated by formulating a robust numerical methodology with predictive capabilities of flow-induced platelet activation. In this study, a phenomenological model for platelet cumulative damage, identified by means of genetic algorithms (GAs), was correlated with *in vitro* experiments conducted in a Hemodynamic Shearing Device (HSD). Platelets were uniformly exposed to flow shear representing the lower end of the stress levels encountered in devices, and platelet activity state (PAS) was measured in response to six dynamic shear stress waveforms representing repeated passages through a device, and correlated to the predictions of the damage accumulation model. Experimental results demonstrated an increase in PAS with a decrease in “relaxation” time between pulses. The model predictions were in very good agreement with the experimental results.

A recognized feature of the complex interplay regulating the pathogenesis of thrombosis is the effect of blood flow-induced mechanical forces on platelets. Physical agonists, such as these flow-induced forces, and chemical agonists, such as adenosine diphosphate and serotonin, trigger platelet activation. This process commences with the secretion of procoagulant and self-stimulating substances from granules,[1] which catalyze thrombin production.[2] As a direct consequence of activation, the platelets undergo a change in shape, marked by pseudopod extension. This increases the strength of adhesion to exogenous surfaces and decreases the resistance to aggregation.

One of the major culprits in blood recirculating devices is the emergence of nonphysiologic (pathologic) flow patterns that enhance the hemostatic response. Elevated flow stresses that are present in the nonphysiologic geometries of blood recirculating devices enhance their propensity to initiate thromboembolism. In recent years, it has been demonstrated that flow induced thrombogenicity, caused by chronic platelet activation and the initiation of thrombus formation, is the salient aspect of mechanically induced blood trauma in devices.[3] This lends itself to the hypothesis that thromboembolism in prosthetic blood recirculating devices is

Reprint Requests: Danny Bluestein, PhD, HSC T18-030, Stony Brook University, Stony Brook, NY 11794-8181.

initiated and maintained primarily by the nonphysiological flow patterns and stresses that activate and enhance the aggregation of blood platelets, increasing the risk of thromboembolism and cardio-embolic stroke.[4]

Within the inherent design constraints of blood recirculating devices and their functionality, minimizing the thrombogenicity of the device is probably the most important design goal. Presently there appears to be no suitable animal model for the monitoring of shear-induced events to reliably predict the onset of physiopathological events in flowing blood or blood vessels.[5] Therefore, progress can be achieved by improving existing *in vitro* and numerical capabilities. Clearly, a modeling approach represents an efficient way to economically test design modifications in devices to realize whether they indeed achieve this design goal. Such an approach should incorporate a model accounting for cellular trauma by means of an activation/damage accumulation hypothesis.[6] Recently, our group has published a comparison of the hemodynamic and thrombogenic performance of two bileaflet mechanical heart valve (MHV) using fluid structure interaction (FSI) modeling that involved the computation of damage accumulation along the trajectories of 15,000 platelets.[7]

Correctly implemented, a physically consistent mathematical model for predicting the effects of fluid shear stress on platelets may lead to a better understanding of the phenomenology of thrombosis. However, because of the complexity and the variety of phenomena involved in blood damage, a universal approach to the problem is incongruous.[8] A successful approach in which an analytic formulation was based on empirically calibrated parameters has been previously demonstrated to predict hemolysis in prosthetic heart valves.[9]

There are many established methods for the *in vitro* investigation of platelet activation.[10,11] Most evaluate the thrombogenic potential in the presence of a mechanical load by measuring the platelet activation state (PAS), but in many cases, those techniques are not sensitive enough to measure minute flow-induced effects, or are limited to very specific aspects of platelet activation. Moreover, because of the inherent variability in blood sources, performance of *in vitro* studies and subsequent analysis and comparison of results can be problematic. For example, different species blood (human *vs.* animals) used for testing thrombogenicity show differences in mechanical fragility and rheological behavior.[12]

In vivo mechanical forces generated by blood flow on platelets during their transit through vessels or devices are quite different from most of the well-defined, controlled-stress conditions applied *in vitro*. Consequently, it is difficult to appropriately assess the activation state of moving platelets under well defined unsteady blood flow conditions predominating vascular pathologies and flow through devices. Such experimental conditions should account for the time-varying loading history and incorporate cumulative effects of the periodic loading.

In this study, we use a computer-controlled hemodynamic shearing device (HSD) that is capable of emulating device and cardiovascular pathologies hemodynamics while uniformly exposing platelets to dynamic shear stress waveforms. The measured platelet activity results are compared to the predictions of a mathematical model proposed by Grigioni *et al*.,[5] which fulfils the requirements for physical consistence[8] and accounts for the cumulative load history effect under time-varying shear conditions. This model employs a Genetic Algorithm-based parameter estimation strategy to identify an optimal model of shear-induced platelet response.

Materials and Methods

In Vitro Studies

Informed consent was obtained from healthy adult volunteers who had not taken aspirin or ibuprofen for 2 weeks. Whole blood, 30 ml, was drawn by venipuncture and collected in 0.3

ml 40% trisodium citrate and centrifuged at 450*g* for 4.5 minutes to prepare platelet-rich plasma (PRP). PRP, 12 ml, was filtered through a 220 ml column of Sepharose 2B beads (2% agarose; Amersham-Pharmacia, Sigma Chemical, St. Louis, MO) to obtain gel-filtered platelets (GFP), as described previously.[13,14] The platelets were diluted to 50,000/μl final concentration in platelet buffer, a Hepes-modified Ca^{2+}-free Tyrodes buffer with 0.1% bovine serum albumin, and 3 mM $CaCl_2$ added 10 minutes prior to experimentation.

Platelets were exposed to shear stress in the HSD, a modified and improved design of the system by Blackman *et al*.,[15] which is capable of reproducing the dynamic aspects of a specified loading waveform with great accuracy. The HSD combines cone-and-plate and Couette viscometer features, as shown in Figure 1. The system was designed such that the shear stresses in both the cone-and-plate and Couette regions are equal, according to

$$\begin{aligned} &\tau_{Cone-Plate}=\tau_{Couette} \rightarrow \\ &\mu\frac{\omega}{\alpha}=2\mu\frac{\omega Ro^2Ri^2}{Ro^2-Ri^2}\left(\frac{1}{r^2}\right)\Big|_{r=Ri} \Rightarrow \alpha=\frac{1}{2}\left[1-\left(\frac{\mathrm{Ri}}{\mathrm{Ro}}\right)^2\right] \\ &(\text{small}\ \alpha, (\mathrm{Ri}/\mathrm{Ro}) \rightarrow 1) \end{aligned} \quad (1)$$

where μ is the viscosity, 1 cP; ω is the angular velocity of the cone; α is the cone angle; and *Ro* and *Ri* are the inner radius of the outer ring and outer radius of the cone, respectively. The design resulted in a 2° cone that is lowered to 10 μm above the stationary plate using a micrometer and a narrow Couette annulus (720 μm gap width). Previous studies in cone-and-plate viscometers under periodical acceleration/deceleration indicate that while oscillation does to some extent destroy the uniformity of shear stress, this may be kept to a minimum by keeping the modified Reynolds number ($Re = (r^2\omega\alpha^2)/(12\,\nu)$—combining the Reynolds and Womersley numbers, (which account for the influences of the local acceleration and centripetal force, respectively) below the limit of secondary flow effects.[16–18] Additional potential effects of higher shear stresses formed at the blood-air interface of the concentric Couette part of the HSD are negligible, as those become apparent only at shear stress levels of several thousands[19]

We have tested our HSD system under more extreme conditions than those presented in the current work, and compared it to steady shear stress experiments in the same system. Our unique design enables generating shear stresses of up to 75 dynes/cm^2 before any noticeable secondary flow effects (Re <0.5; where these effects become apparent). We have further demonstrated in this system that triangular loading waveforms (peaking at 100 dynes/cm^2) with root mean square (RMS) values representing a corresponding constant shear stress value produced the same platelet activation level as the constant shear stress (both measured with PAS—no statistically significant differences).[20]

The blood-contacting surfaces were manufactured from blood compatible ultra-high molecular weight polyethylene (UHMWPE) and treated with silicone 10 minutes prior to experiments. Dynamic shear stress waveforms were simulated by the means of a computerized stepper motor (VS23B, Compumotor Division, Parker Hannifin Corporation, Rohnert Park, CA), programmed with the supplied Motion Architect software, and transferred via the ZETA6104 microstepping drive.

Triangular and square waveforms (Figure 2) were applied to simulate repeated passages through a generic device. Each waveform had a baseline shear of 1.5 dynes/cm^2, imposed for a time period of T2, and peak shear of 20 dynes/cm^2, for a period of T1. The total acceleration and deceleration time T_{ad} was 1 second. For the triangular waveform, T1 was 0 seconds, while for the square waveform, T1 was 2.5 seconds. For each type of waveform, three T2 periods

(10, 30, and 60 seconds) were applied. Each experiment was conducted for 60 minutes, with platelet samples taken every 5 minutes for 30 minutes, and then every 15 minutes thereafter. For each of the six waveforms, five runs were conducted.

Platelet activation state (PAS) was quantified using the chemically modified prothrombinase-based assay developed by Jesty and Bluestein,[21] which uses acetylated prothrombin, and the thrombogenic potential quantified by measuring thrombin generation rates.[13,22] Unlike cytometry markers that quantify very specific aspects of platelets activation, PAS quantifies the more global thrombogenic aspect of platelet prothrombinase activity, *i.e.*, its contribution to thrombin generation—an actual clotting inducing product. The PAS assay was successfully applied for measuring the procoagulant activity of devices, both *in vitro* and in an animal model,[23–25] and under various shear stress-exposure time combinations in flow loops and stenosis models.[22,26] PAS values were normalized against the average activity of fully activated platelets measured for each experiment, obtained by sonication (10 W for 10 seconds, Branson Sonifier 150 with microprobe, Branson, MO). PAS values are expressed as a fraction of maximal prothrombinase activity. Statistics were conducted using the Student's *t* test for each set of T1 values, where T2 = 60 seconds was considered the control for each set. Time courses of PAS *vs*. time were fitted to a quadratic equation, $PAS_{ie} = \alpha t^2 + \beta t + \gamma$, and the square coefficient, α, was used as an index of curvature. This is the rate of increase in platelet activation rate. To determine whether activation was significantly nonlinear the means (±SD) of α were tested against the null hypothesis of linear activation, *i.e.*, $\alpha = 0$, using a modified form of Student's *t* test, $t = (\bar{x} - \mu)/(s\sqrt{n})$, where $\bar{x}$ is the mean observed α, *s* its standard deviation, *n* the degrees of freedom, and μ is the null-hypothesis value against which we test.

Damage Accumulation Model

A model describing damage of formed elements in blood requires establishment of a correlation between the mechanical loading history $\tau(t)$, the exposure time (t) and the phenomenological response of the formed elements. This general relationship can be expressed as:

$$dBD = f(\tau[t_0 \ldots\ldots t], dt) \tag{2}$$

where *dBD* is the generic blood damage rate, and t_0 is the time at the beginning of the observation.

In this study, the novel Lagrangian-based mathematical model proposed by Grigioni *et al*.[5] was adopted. It is based on the damage theory articulated by Equation 2 and reflects the cumulative damage sustained by formed elements exposed to time-dependent stress levels.

Originally developed for the evaluation of RBC hemolysis, this model was adapted for the assessment of PAS, since platelet activation under dynamic loading exhibits similar characteristics.[1] Specifically, it is expressed as

$$dPAS = Ca\left(\int_{t_0}^{t} \tau(\xi)^{b/a} d\xi + \frac{PAS(t_0)^{1/a}}{C}\right)^{a-1} \tau(t)^{b/a} dt \tag{3}$$

where *dPAS* is the infinitesimal contribution to the platelet activation state, $PAS(t_0)$ is the value of platelet activation at the starting time of observation t_0 (*i.e.*, senescence, or previous damage history during previous passages through a prosthetic valve, for example) and (a,b,C) are model constants.

The platelet activation state index can be expressed as the integral sum of the infinitesimal contributions represented by Equation 3:

$$PAS=\int_{t_0}^{t} Ca\left[\int_{t_0}^{\varphi}\tau(\xi)^{b/a}d\xi+\frac{PAS(t_0)^{1/a}}{C}\right]^{a-1}\tau(\varphi)^{b/a}d\varphi \tag{4}$$

The integral sum inside the square brackets in Equation 4 is representative of the mechanical load sustained by the platelets moving along a generic fluid path, made up of the summation of the subsequent elementary contributions to damage acting in each infinitesimal time interval.

With this formulation, it is possible to address the problem of the shear time-varying history experienced by the platelets under dynamic blood flow conditions.

Model Identification Protocol

The model identification process involves the determination of an unknown parameter vector $\mathbf{P} = [a, b, C]^T$. The estimation of the unknown parameters of the model for *PAS* prediction was performed by applying GAs.

GAs are random search algorithms for nonlinear problems based on the rules of natural selection. Their implementation requires the three components of vector **P** to be encoded through a proper representation method. In the study, floating-point representation was chosen. Each individual was composed by three genes, *i.e.*, the three components of vector **P**. The limits of the parameters to be estimated, defining the borders for the field of existence of the solution, were set as

$$a=0-10;b=0-10;C=10^{-12}-10^{-5} \tag{5}$$

To overcome the problem of the possible dependence of the identification procedure on the initial values of the parameters, the genetic algorithm was initiated with 150 randomly generated individuals. An appropriate cost function, the so-called fitness function, was built to control the GA search progress in an acceptable direction.

The model of Equation 2 states that platelet activation time course is predicted by a function of the unknown parameter vector **P**, where

$$PAS_m(t_i,\mathbf{P})=f(t_0,\ldots..t_i,\mathbf{P}) \tag{6}$$

is the estimated value of platelet activation at time t_i ($i = 1,\ldots. N$).

In the model identification procedure, we used the time courses of PAS *vs*. time-fitted to a quadratic equation (previously labeled PAS_{ie}). The difference between the platelet activation fitted data $PAS_{ie} = PAS_{ie1}, PAS_{ie2}, \ldots, PAS_{ieN}]^T$ and the model estimated data $PAS_m = PAS_{m1}, PAS_{m2}, \ldots, PAS_{mN}]^T$ can be written in terms of square error sum as:

$$\Theta=\sum_{i=1}^{N}(PAS_m(t_i)-PAS_{ie}(t_i))^2 \tag{7}$$

where N is the number of measured points. The estimation of the unknown parameter vector **P** was considered the objective of the GA identification process. This was optimized through the minimization of the cost function:

$$\Psi=\sum_{k=1}^{M}\Theta_k \tag{8}$$

where θ_k is the mean square error, as given by Equation 8, between the experimentally measured *PAS* and the *PAS* predicted by Equation 3, and k is the number of the loading histories imposed. The four loading histories with T2 period equal to 10 and 30 seconds were used for the model identification while the triangular load history with T2 = 60 seconds was excluded since its activation level was negligible ($PAS_{max} = 0.066 \pm 0.021$). The remaining loading curve (T1 = 2.5 and T2 = 60 seconds) was used as a test case for the model.

The performance evaluation was translated in a scalar fitness value *ff* as follows:

$$ff=D-\Psi \tag{9}$$

where D is a large positive constant parameter (accomplishing the transformation of the minimization problem into a maximization problem.,[27] as requested by GAs). The quality of each solution, the estimated vector **P**, was evaluated by:

$$\widehat{\mathbf{P}}=arg_p\,max(ff)=arg_p\,max(D-\Psi)=$$
$$arg_p\,max\left(D-\sum_{i=1}^{N}[PAS_m(t_i)-PAS_{ie}(t_i)]^2\right) \tag{10}$$

After a fitness criterion is applied to the solution space, the new generation is constructed from the actual population by applying three genetic operators: reproduction, mutation and crossover (details can be found in Goldberg[28]).

The steps of a GA are summarized in Figure 3. The number of iterations required for convergence to the desired evolution was set at 2000 after a sensitivity study (data not shown). To avoid converging to a local minimum, the cycle was repeated 200 times, thus obtaining 200 solutions. Among the solutions, parameter vector $\hat{\mathbf{P}}$ maximizing the fitness function, Equation 9, was considered the best estimate of vector **P**.

The numerical implementation of the methodology described above was performed using an in-house developed code written with MATLAB programming language (Math-Works, Natick, MA).

Results

Mean *PAS* normalized experimental data for triangular shear stress waveforms are shown in Figure 4. A higher normalized *PAS* value was observed for T2 = 10 seconds, as compared to T2 = 30 seconds and T2 = 60 seconds. For T2 = 10 seconds, mean *PAS* at 60 minutes was 0.285 ± 0.189 (SEM), while for T2 = 60 seconds, this was 0.067 ± 0.021 (SEM). A similar observation was made for square shear stress waveforms at the 60-minute mark, as shown in Figure 5, with mean *PAS* 0.341 ± 0.133 (SEM) for T2 = 10 seconds, while the mean *PAS* for T2 = 60 seconds was 0.236 ± 0.058 (SEM). As with the triangular waveforms, five runs were conducted for each T2 condition for the square shear stress waveforms. Increased variability in *PAS* values

for lower T2 (10 and 30 seconds) are observed, potentially because of unsteady flow immediately after deceleration from peak to baseline shear conditions. For all conditions, although not statistically significant ($p > 0.05$), the results show that decreased "relaxation" time (T2) between shear stress pulses leads to increased platelet activation rate. Furthermore, mean *PAS* values for the square waveforms were observed to be higher than those for triangular waveforms at the same T2.

Mean *PAS* normalized data used in the present study and the corresponding model-derived curve fits are shown in Figure 6. The GA-based identification procedure converged to a vector **P** with model parameters given by $a = 1.3198$; $b = 0.6256$; $C = 10^{-5}$

The mathematical model fine-tuned by GAs yields *PAS* values that were in very good agreement with the experimental results. The comparison between the model predictions and experimental results clearly demonstrates that the *PAS* value, as predicted by Equation 5, is sensitive to platelet response under time-varying shear stress for both the triangular and the square shear stress waveforms. Moreover, the model was able to capture the distinctive nonlinear *PAS* trend and its concavity.

The agreement between the *PAS* measurements and the model descriptions was better for the square waveforms, as evident from the relative root mean square error (RRMS) values. For T2 = 10 seconds the RRMS values were square_ RRMS = 0.446 *vs.* triang_RRMS = 0.628, and for the case of T2 = 30 seconds the values were square_RRMS = 0.267 *vs.* triang_RRMS = 0.910. This behavior may be the consequence of the sensitivity of the model to shear stress levels applied for a longer duration (*e.g.*, the duty cycle $(T1 + T_{ad})/(T1 + T_{ad} + T2)$ of the square shear history is greater than the triangular one).

Figure 7 shows the *PAS* predicted by the identified model ($a = 1.3198$; $b = 0.6256$; $C = 10^{-5}$) in response to a square shear waveform that was not used in the identification procedure (relaxation period T2 = 60 seconds). The strong correlation between the *in vitro* experimental results and the model's results reinforces the model predictive capabilities.

Discussion

The present work is focused on the effect of mechanical loading on platelet activation, and the cumulative effect of repeated exposure to this loading. Early literature regarding the effects of bulk shear stress on platelets indicate that shear stress directly activates platelets.[11,29,30] Some investigators hypothesized that shear stress did not directly activate platelets, rather RBC and platelet lysis that increases extracellular concentrations of stored platelet agonists, particularly adenosine diphosphate (ADP), subsequently activating the remaining platelets.[31,32] However, Moake *et al.*[33] demonstrated, based on previous studies using flow systems,[34–37] that platelet aggregation in response to pathologically elevated shear stress is not an artifact of cell lysis.

To directly evaluate the effects of bulk fluid shear stress on platelets, it is first necessary to eliminate as thoroughly as possible, all platelet-surface interactions. Platelet-surface interactions can be minimized by coating the shear stress-generating surfaces with silicone or another nonthrombogenic material. This results in platelet response to shear remaining nearly constant over a large range of surface to volume ratio.[11,38,39] The use of blood compatible materials and silicone-coated surfaces in our HSD system guaranteed a reliable *in vitro* system for measuring platelet response to direct shear. Higher variability in *PAS* values that was observed for the more dynamic waveforms (*i.e.*, shorter T2 between pulses) may be attributed to the potential appearance of transient vortices during the abrupt deceleration from peak to the baseline shear. Such vortical structures would tend to increase collision rates among quiescent and activated platelets and may temporarily enhance aggregation.

We have compared the results from the present study to previously published data in the similar shear stress ranges under constant shear flow. Platelets in platelet-rich plasma (PRP) sheared at 20 dynes/cm^2 for 60 seconds showed approximately 3% activation, as measured by CD62P expression.[40] This value is higher than the 1.65% to 1.67% activation for the 5-minute samples in our T1 = 0 seconds waveform experiments, which shows that constant shear stress yields higher activation values than variable shear stress, where platelets are exposed to a higher value for only a fraction of the total exposure time. Furthermore, platelets in whole blood exposed to a constant shear rate 420 s^{-1} (corresponding to a shear stress of 14.7 dynes/cm^2, assuming whole blood viscosity of 3.5 cP) did not express a significant increase in GP IIb/IIIa activation (approximately 1%) at 4.5 minutes, whereas Annexin V binding was detected to be 1.5% to 2%.[41] It should also be emphasized that the platelet counts for these prior studies are higher than the 50,000/μl utilized in the present study, which may yield lower *PAS* values. However, because of the short experimental duration of most prior studies (*i.e.*, 1–4.5 minutes), difference in *PAS* values due to platelet count is not evident. In the past, we have published results in flow in a flow loop under intermittent shear stress.[22] In that study, platelets exposed to shear stresses of 11 and 33 dynes/cm^2 in a 1-m stenotic flow loop showed a 3.8-fold increase in activation rate (0.0024–0.0090 min^{-1}) in a 30-minute time frame. The stenotic region had an exposure time fraction of 24% to the higher shear stress, with the remaining time entailing an exposure to 1.4 dynes/cm^2. The linear portion of the slopes for our T1 = 0 seconds experiments yielded values of 0.0013, 0.0016, and 0.0051 min^{-1} for T2 values of 60, 30, and 10 seconds, respectively. These correspond to exposure time fractions to high shear stress (20 dynes/cm^2) of 1.6%, 3.2%, and 9.9%, respectively. The results from the previous studies reinforce the validity of the current study using the PAS assay utilizing variable shear stresses in our HSD system.

Recently, some intricacies involving the relationship between coefficients of power-law based mathematical models for red blood cell damage and experimental data were identified.[42] It was indicated that the functional relationship could be fine-tuned by readjusting the coefficients in the formula according to *in vitro* data. It was concluded that the coefficients in the trauma prediction equations were not universal, rather depending on the flow conditions and may be valid only for predominantly laminar flows.[43]

Considering that under a given shear stress load history there will be a given rate of consumption of resting platelets, and that once fully activated those platelets cannot be activated anymore, the shear stress will progressively apply only to a residual population of the remaining quiescent platelets. Accordingly, as observed with sheared red blood cells,[44] the progression of platelet activation state is expected to exhibit a similar asymptotic behavior. In the present study, we have demonstrated that the model predictions are consistent with the experimental results at activation levels lower than 0.35. However, for cases in which high consumption rates are expected, we are confident that the power-law model of Equation 4 will be able to capture the asymptotic behavior in the intermediate to large damage accumulation range while approaching full platelet activation (as the one expected at shear stress values characterizing prosthetic mechanical heart valves).[45]

A global identification approach was selected over a local routine [*e.g.*, Nonlinear Least Square (NLS) method], because the latter is notorious for getting trapped in local minima when applied to nonlinear problems that characterize biomechanics, or prove unsuitable due to the required model parameters initialization. GA, the global identification approach used in this study, overcomes the need of setting the initial values for the model parameters by searching the parameter space in a controlled random fashion thus allowing exploration of a wider solution space (Equation 5).

Although the work presented in our study demonstrates a model accounting for blood trauma for predicting device thrombogenicity, it requires further experiments where blood samples are exposed to dynamic flow field conditions under controlled, time-varying shear. Exposure to the different dynamic flow conditions allows the identification of coefficients that can be empirically calibrated with respect to the characteristic flow conditions in the device. The inherent difficulties in designing experimental studies in this field were pointed out by other researchers.[43]

The shear stress levels tested here represent only the lower end of those found in devices, but the results of the current study are still relevant to devices. The main utility of this work was to test the predictions of an innovative damage model based on genetic algorithms that is aimed at predicting cumulative damage and platelet activation during repeated passages in devices. One should keep in mind that the bulk platelets flowing in devices do not patently flow through the higher stress regions. Yet, with repeated passages, the platelets sustain damage accumulation that significantly contributes to the thrombogenic potential of the device in the longer run.[46] Following the successful implementation of the GA-based model in our HSD with artificial loading waveforms, we plan to apply this model and fine-tune its parameters to correlate its predictions with our ongoing platelet activity measurements in devices (various PHV mounted in a LVAD recirculation loop). We plan to do it in a complementary fashion, by directly measuring platelet activity in the devices themselves, and by extracting typical shear stress waveforms from numerical simulations of flow in the devices and applying them as a bulk load waveform to a platelet population in the HSD apparatus.

Although applied to only a few synthetic load histories, we feel confident that the model will be able to predict the thrombogenic potential of implantable devices, such as prosthetic heart valves and blood pumps, by obtaining typical shear histories from computational fluid dynamics modeling. Our future studies in the HSD will use those as the input loading waveforms to bring the shear stress levels and exposure time combinations closer to those found in devices.

Acknowledgments

The authors gratefully thank Dr. Jolyon Jesty for his advice on experiments and Mrs. Sulan Xu for her assistance during experiments. This study was supported by an Established Investigator Award from the American Heart Association (Award No. 0340143N, DB) and the National Science Foundation (Award No. 0302275, DB).

References

1. Hellums JD. 1993 Whitaker Lecture: Biorheology in thrombosis research. Ann Biomed Eng 1994;22:445–455. [PubMed: 7825747]
2. Colman RW. Chapter 3: Mechanisms of thrombus formation and dissolution. Cardiovasc Pathol 1993;2:23–31.
3. Travis BR, Marzec UM, Ellis JT. The sensitivity of indicators of thrombosis initiation to a bileaflet prosthesis leakage stimulus. J Heart Valve Dis 2001;10:228–238. [PubMed: 11297211]
4. Bluestein D. Research approaches for studying flow induced thromboembolic complications in blood recirculating devices. Expert Rev Med Devices 2004;1:65–80. [PubMed: 16293011]
5. Grigioni M, Morbiducci U, D'Avenio G, et al. A novel formulation for blood trauma prediction by a modified power-law mathematical model. Biomech Model Mechanobiol 2005;4:249–260. [PubMed: 16283225]
6. Bluestein D. Towards optimization of the thrombogenic potential of blood recirculating cardiovascular devices using modeling approaches. Expert Rev Med Devices 2006;3:267–270. [PubMed: 16681446]
7. Dumont K, Vierendeels J, Kaminsky R, et al. Comparison of the hemodynamic and thrombogenic performance of two bileaflet mechanical heart valves using a CFD/FSI model. J Biomech Eng 2007;129:558–565. [PubMed: 17655477]

8. Grigioni M, Daniele C, Morbiducci U, et al. The power-law mathematical model for blood damage prediction: Analytical developments and physical inconsistencies. Artif Organs 2004;28:467–475. [PubMed: 15113341]
9. Giersiepen M, Wurzinger LJ, Opitz R, Reul H. Estimation of shear stress-related blood damage in heart valve prostheses—In vitro comparison of 25 aortic valves. Int J Artif Organs 1990;13:300–306. [PubMed: 2365485]
10. Born GV. Aggregation of blood platelets by adenosine diphosphate and its reversal. Nature 1962;194:927–929. [PubMed: 13871375]
11. Anderson GH, Hellums JD, Moake J, Alfrey CP Jr. Platelet response to shear stress: Changes in serotonin uptake, serotonin release, and ADP induced aggregation. Thromb Res 1978;13:1039–1047. [PubMed: 749261]
12. Blackshear PL Jr, Forstrom RJ. Comparative mechanical blood properties. DHEW Publication 1973;72:525–539.
13. Schulz-Heik K, Ramachandran J, Bluestein D, Jesty J. The extent of platelet activation under shear depends on platelet count: Differential expression of anionic phospholipid and factor Va. Pathophysiol Haemost Thromb 2005;34:255–62. [PubMed: 16772736]
14. Yin W, Gallocher S, Pinchuk L, et al. Flow-induced platelet activation in a St. Jude mechanical heart valve, a trileaflet polymeric heart valve, and a St. Jude tissue valve. Artif Organs 2005;29:826–831. [PubMed: 16185345]
15. Blackman BR, Garcia-Cardena G, Gimbrone MA Jr. A new in vitro model to evaluate differential responses of endothelial cells to simulated arterial shear stress waveforms. J Biomech Eng 2002;124:397–407. [PubMed: 12188206]
16. Chung CA, Tzou MR, Ho RW. Oscillatory flow in a cone-and-plate bioreactor. J Biomech Eng 2005;127:601–610. [PubMed: 16121530]
17. Shankaran H, Neelamegham S. Effect of secondary flow on biological experiments in the cone-plate viscometer: Methods for estimating collision frequency, wall shear stress and inter-particle interactions in non-linear flow. Biorheology 2001;38:275–304. [PubMed: 11673645]
18. Shankaran H, Neelamegham S. Nonlinear flow affects hydrodynamic forces and neutrophil adhesion rates in cone-plate viscometers. Biophys J 2001;80:2631–2648. [PubMed: 11371440]
19. Leverett LB, Hellums JD, Alfrey CP, Lynch EC. Red blood cell damage by shear stress. Biophys J 1972;12:257–73. [PubMed: 5016112]
20. Yin, W. PhD Dissertation. Stony Brook, NY: State University of New York at Stony Brook; 2004. Flow Induced Platelet Activation in Mechanical Heart Valves—In Vitro, In Vivo and Numerical Studies.
21. Jesty J, Bluestein D. Acetylated prothrombin as a substrate in the measurement of the procoagulant activity of platelets: Elimination of the feedback activation of platelets by thrombin. Anal Biochem 1999;272:64–70. [PubMed: 10405294]
22. Jesty J, Yin W, Perrotta P, Bluestein D. Platelet activation in a circulating flow loop: Combined effects of shear stress and exposure time. Platelets 2003;14:143–149. [PubMed: 12850838]
23. Bluestein D, Yin W, Affeld K, Jesty J. Flow-Induced Platelet Activation in a Mechanical Heart Valve. J Heart Valve Dis 2004;13:501–508. [PubMed: 15222299]
24. Yin W, Alemu Y, Affeld K, et al. Flow-induced platelet activation in bileaflet and monoleaflet mechanical heart valves. Ann Biomed Eng 2004;32:1058–1066. [PubMed: 15446502]
25. Yin W, Krukenkamp IB, Saltman AE, et al. The Thrombogenic Performance of a St. Jude Bileaflet MHV in a Sheep Model. ASAIO J 2006;52:28–33. [PubMed: 16436887]
26. Raz S, Einav S, Alemu Y, Bluestein D. DPIV prediction of flow induced platelet activation-comparison to numerical predictions. Ann Biomed Eng 2007;35:493–504. [PubMed: 17286206]
27. Morbiducci U, Di Benedetto G, Kautzky-Willer A, et al. Improved usability of the minimal model of insulin sensitivity based on an automated approach and genetic algorithms for parameter estimation. Clin Sci (Lond) 2007;112:257–263. [PubMed: 16961464]
28. Goldberg, DE., editor. Genetic Algorithms in Search, Optimization and Machine Learning. New York: Addison Wesley; 1989.
29. Brown CH III, Leverett LB, Lewis CW, et al. Morphological, biochemical, and functional changes in human platelets subjected to shear stress. J Lab Clin Med 1975;86:462–471. [PubMed: 1151161]

30. Anderson GH, Hellums JD, Moake JL, Alfrey CP Jr. Platelet lysis and aggregation in shear fields. Blood Cells 1978;4:499–511. [PubMed: 162570]

31. Wurzinger LJ, Opitz R, Wolf M, Schmid-Schonbein H. “Shear induced platelet activation”—A critical reappraisal. Biorheology 1985;22:399–413. [PubMed: 2937464]

32. Kroll MH, Hellums JD, McIntire LV, et al. Platelets and shear stress. Blood 1996;88:1525–1541. [PubMed: 8781407]

33. Moake JL, Turner NA, Stathopoulos NA, et al. Involvement of large plasma von Willebrand factor (vWF) multimers and unusually large vWF forms derived from endothelial cells in shear stress-induced platelet aggregation. J Clin Invest 1986;78:1456–1461. [PubMed: 3491092]

34. Sixma JJ, Sakariassen KS, Beeser-Visser NH, et al. Adhesion of platelets to human artery subendothelium: Effect of factor VIII-von Willebrand factor of various multimeric composition. Blood 1984;63:128–139. [PubMed: 6418228]

35. Turitto VT, Weiss HJ, Baumgartner HR. Decreased platelet adhesion on vessel segments in von Willebrand’s disease: A defect in initial platelet attachment. J Lab Clin Med 1983;102:551–564. [PubMed: 6413629]

36. Turitto VT, Weiss HJ, Baumgartner HR. Platelet interaction with rabbit subendothelium in von Willebrand’s disease: Altered thrombus formation distinct from defective platelet adhesion. J Clin Invest 1984;74:1730–1741. [PubMed: 6334102]

37. Turitto VT, Weiss HJ, Zimmerman TS, Sussman II. Factor VIII/von Willebrand factor in subendothelium mediates platelet adhesion. Blood 1985;65:823–831. [PubMed: 3872140]

38. Baumgartner HR, Tschopp TB, Meyer D. Shear rate dependent inhibition of platelet adhesion and aggregation on collagenous surfaces by antibodies to human factor VIII/von Willebrand factor. Br J Haematol 1980;44:127–139. [PubMed: 6769457]

39. Belval T, Hellums JD, Solis RT. The kinetics of platelet aggregation induced by fluid-shearing stress. Microvasc Res 1984;28:279–288. [PubMed: 6521656]

40. Zhang JN, Bergeron AL, Yu Q. Duration of exposure to high fluid shear stress is critical in shear-induced platelet activation-aggregation. Thromb Haemost 2003;90:672–678. [PubMed: 14515188]

41. Holme PA, Orvim U, Hamers MJ. Shear-induced platelet activation and platelet microparticle formation at blood flow conditions as in arteries with a severe stenosis. Arterioscler Thromb Vasc Biol 1997;17:646–653. [PubMed: 9108776]

42. Paul R, Marseille O, Hintze E. In vitro thrombogenicity testing of artificial organs. Int J Artif Organs 1998;21:548–552. [PubMed: 9828061]

43. De Wachter D, Verdonck P. Numerical calculation of hemolysis levels in peripheral hemodialysis cannulas. Artif Organs 2002;26:576–582. [PubMed: 12081515]

44. Farinas MI, Garon A, Lacasse D, N’Dri D. Asymptotically consistent numerical approximation of hemolysis. J Biomech Eng 2006;128:688–696. [PubMed: 16995755]

45. Alemu Y, Bluestein D. Flow induced platelet activation and damage accumulation in a mechanical heart valve- numerical studies. Artif Organs 2007;31:677–688. [PubMed: 17725695]

46. Dumont K, Vierendeels J, van Nooten G, et al. Comparison of ATS Open Pivot Valve and St Jude Regent Valve using a CFD model based on fluid-structure interaction. J Biomech Eng 2007;129:558–565. [PubMed: 17655477]

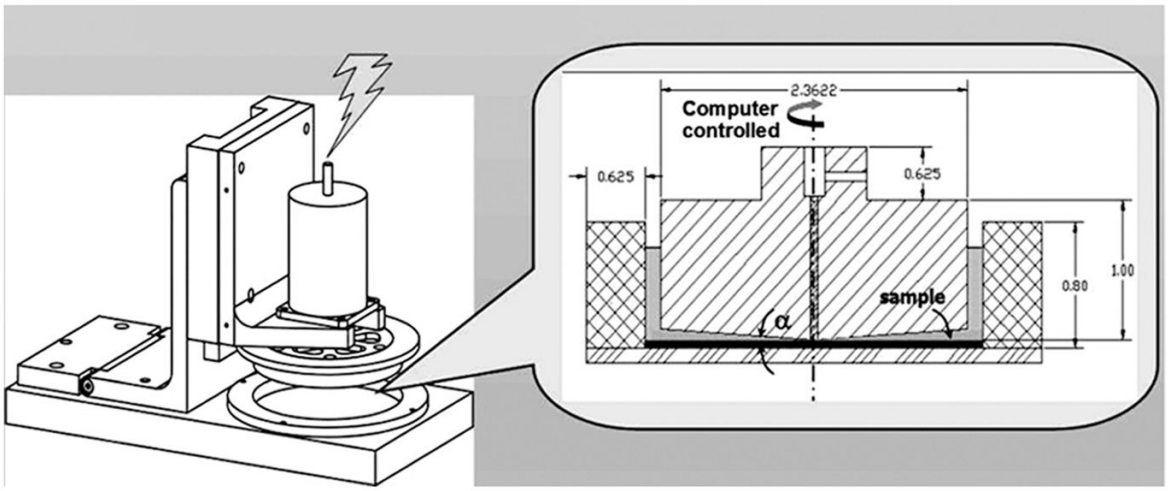

Figure 1.
Hemodynamic shearing device (HSD), consisting of a ring mounted on a stationary plate. Fluid shear stresses are induced by a cone mounted on a computer-controlled stepper motor. Platelet samples for PAS assays are drawn from the Couette region, between the rotating cone and mounted ring.

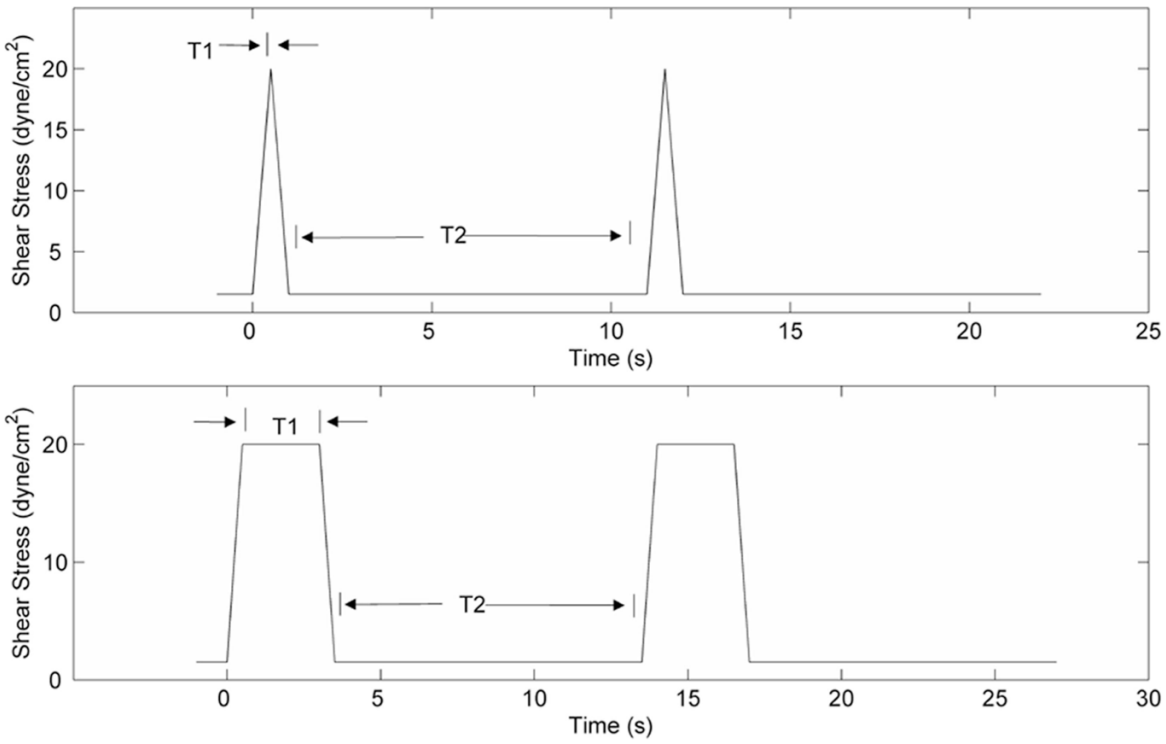

Figure 2.
Triangular (top) and square (bottom) shear stress waveforms utilized in this study. The durations of the peak shear stress, T1, selected were 0 and 2.5 seconds, while the "relaxation" period, T2, had values of 10, 30, and 60 seconds.

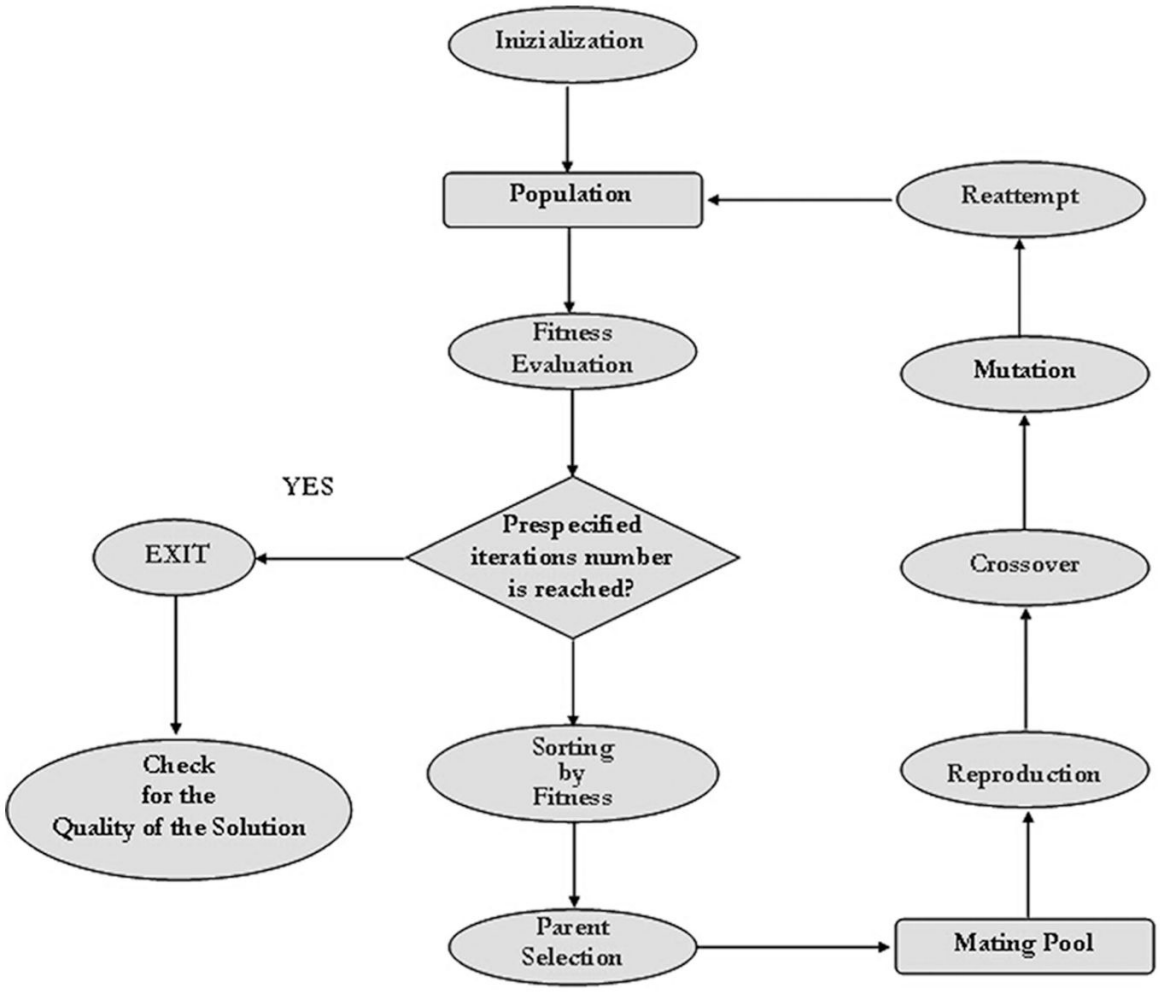

Figure 3.
Flow diagram of the genetic algorithms (GAs) identification methodology. After a random initialization, the fitness function is evaluated on the population generated. The individuals which best accomplish the fitness criteria are selected and a new population is created by mutation, crossover and selection rules. This process is performed until the maximum number of iterations is reached.

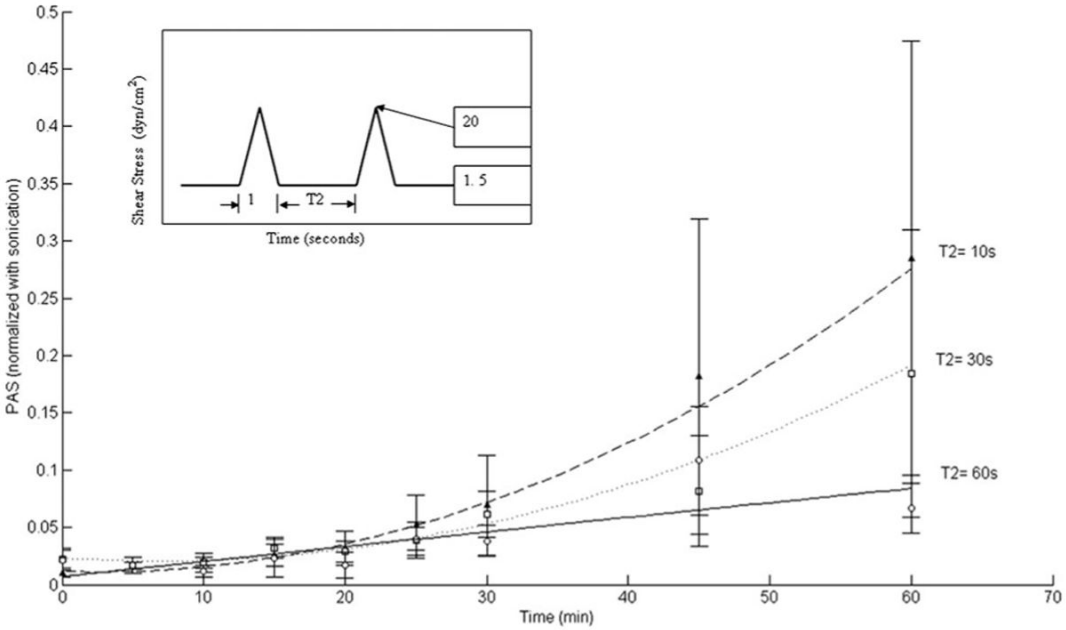

Figure 4.

Normalized *PAS* values for triangular shear stress waveforms. For T2 = 10 s, mean *PAS* at 60 minutes was 0.285 ± 0.189 (SEM), with 0.067 ± 0.021 (SEM) for T2 = 60 seconds and 0.184 ± 0.125 (SEM) for T2 = 30 seconds. While higher mean values are observed for T2 = 10 and 30 seconds, they are not significant ($p > 0.05$).

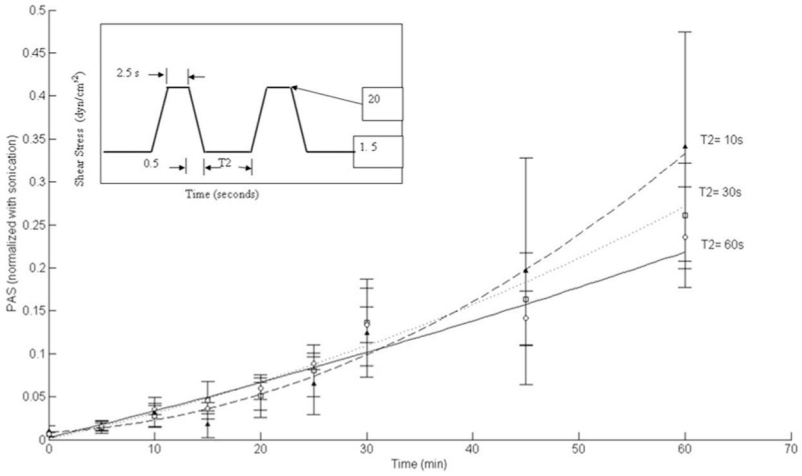

Figure 5.

Normalized *PAS* values for square shear stress waveforms. For T2 = 10 seconds, mean *PAS* at 60 minutes was 0.341 ± 0.133 (SEM), with 0.236 ± 0.058 (SEM) for T2 = 60 seconds and 0.261 ± 0.062(SEM) for T2 = 30 seconds. While higher mean values are observed for T2 = 10 s and 30 s, they are not significant ($p > 0.05$).

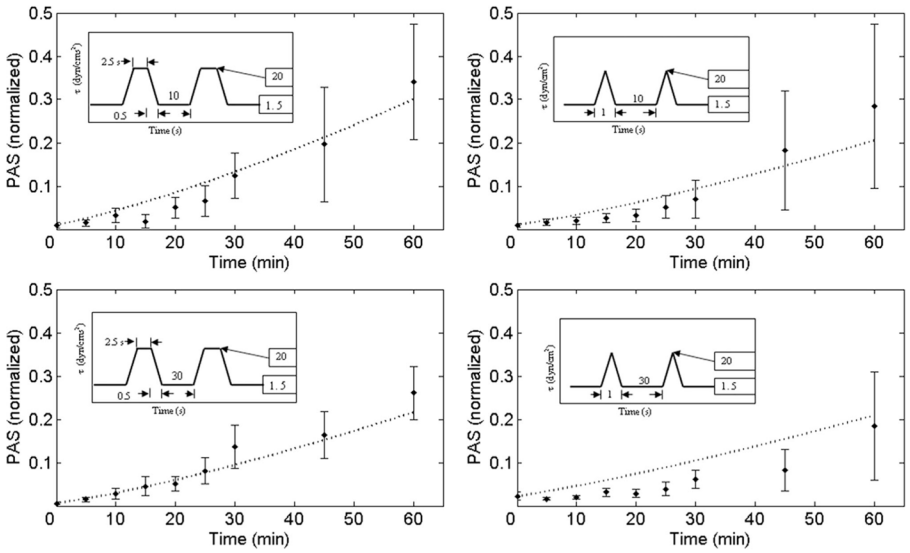

Figure 6.

Model results (dashed lines) compared with experimental values for both square and triangular shear stress waveforms, for T2 = 10 seconds (top) and T2 = 30 seconds (bottom). The model appears to fit the square waveform experimental data better than the triangular waveform data.

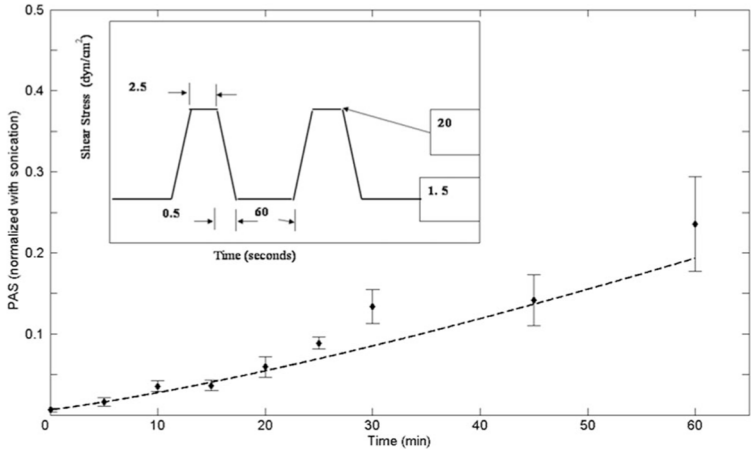

Figure 7.

Model results (dashed lines) compared with experimental values for the square shear stress waveform (T2 = 60 seconds), not employed in the model identification procedure. The model prediction agrees very well with the square waveform experimental data.